ACS NANO

www.acsnano.org

ARTICLE

Amplified Spontaneous Emission from Electron−Hole Quantum Droplets in Colloidal CdSe Nanoplatelets

Nicolas E. Watkins, Benjamin T. Diroll, Kali R. Williams, Yuzi Liu, Chelsie L. Greene, Michael R. Wasielewski, and Richard D. Schaller*

Cite This: https://doi.org/10.1021/acsnano.3c13170

Read Online

ACCESS | Metrics & More | Article Recommendations | Supporting Information

ABSTRACT: Two-dimensional cadmium selenide nanoplatelets (NPLs) exhibit large absorption cross sections and homogeneously broadened band-edge transitions that offer utility in wide-ranging optoelectronic applications. Here, we examine the temperature-dependence of amplified spontaneous emission (ASE) in 4- and 5-monolayer thick NPLs and show that the threshold for close-packed (neat) films decreases with decreasing temperature by a factor of 2−10 relative to ambient temperature owing to extrinsic (trapping) and intrinsic (phonon-derived line width) factors. Interestingly, for pump intensities that exceed the ASE threshold, we find development of intense emission to lower energy in particular provided that the film temperature is ≤200 K. For NPLs diluted in an inert polymer, both biexcitonic ASE and low-energy emission are suppressed, suggesting that described neat-film observables rely upon high chromophore density and rapid, collective processes. Transient emission spectra reveal ultrafast red-shifting with the time of the lower energy emission. Taken together, these findings indicate a previously unreported process of amplified stimulated emission from polyexciton states that is consistent with quantum droplets and constitutes a form of exciton condensate. For studied samples, quantum droplets form provided that roughly 17 meV or less of thermal energy is available, which we hypothesize relates to polyexciton binding energy. Polyexciton ASE can produce pump-fluence-tunable red-shifted ASE even 120 meV lower in energy than biexciton ASE. Our findings convey the importance of biexciton and polyexciton populations in nanoplatelets and show that quantum droplets can exhibit light amplification at significantly lower photon energies than biexcitonic ASE.

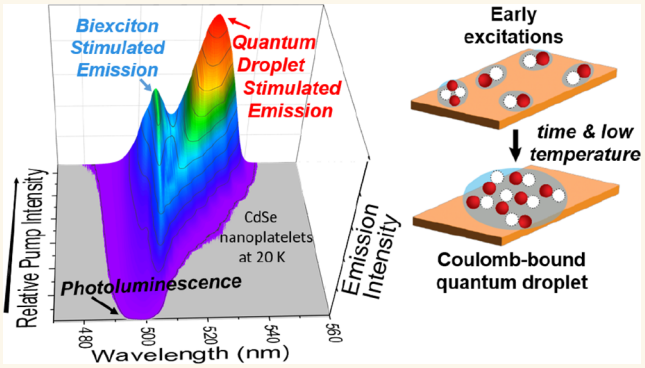

KEYWORDS: *multiple excitons, optical gain, quantum droplet, excited-state dynamics, stimulated emission, exciton condensation*

Colloidally synthesized, two-dimensional CdSe nanoplatelets (NPLs) exhibit thickness-tunable absorption and emission properties that offer potential utility in applications such as high color rendering index light-emitting diodes and solution-processed lasers.[1−5] Routes to monodisperse control over the monolayer (ML) thickness in colloidal NPL ensembles permit the observation of homogeneous line width-dominated radiative recombination that, combined with large absorption cross-section, yields low-threshold amplified spontaneous emission (ASE), high modal gain, and robust laser action.[1,4−9] However, band-edge optical gain and ASE compete with fast nonradiative recombination pathways such as Auger recombination[10−13] and carrier trapping that have motivated continued research efforts.[14−16]

CdSe NPLs, like several other 2D semiconductors,[17−19] engender large exciton binding energies in the range of 100 to 400 meV,[20−23] which approach 25 times the bulk semiconductor value and significantly exceed available thermal energy at room temperature. As a result of quantum confinement and reduced dielectric screening, electron−hole pairs in NPLs form excitons at room temperature rather than independent charge carriers. A continuous density of states and typical phonon line width broadening in NPLs ($\Gamma = \Gamma_0 + \Gamma_{phonon}(T)$) suggests that ASE could exhibit temperature-

Received: December 29, 2023
Revised: March 1, 2024
Accepted: March 7, 2024

dependent threshold as reduced thermal energy serves to focus excitons into a narrower distribution of states, also apparent, e.g., in temperature-dependent photoluminescence (PL)[3] and carrier cooling studies.[24] At the same time, introduction of a second electron−hole pair within the same particle can result in either two independent free excitons with an uncorrelated center of mass motion, or one biexciton (which is sometimes termed an exciton molecule),[25−27] provided that the biexciton Coulomb binding energy exceeds available thermal energy. Under conditions that the biexciton binding energy is comparable to available thermal energy, free excitons and biexcitons experience a quasi-equilibrium population distribution as described recently.[25,28] Biexcitons exhibit 20−45 meV binding energies relative to free excitons for the particles studied herein, which is an order of magnitude weaker than the exciton binding energy.[25,29] Both exciton and multiexciton behaviors in 2D NPLs, thus, differ fundamentally from 0D quantum dots, wherein two electron hole pairs necessarily spatially overlap in a 0D particle that is smaller than the Bohr radius, irrespective of the biexciton binding energy.[30] Furthermore, as the number of photoexcited electron−hole pairs in a NPL increases above two, polyexciton (PE) many-body states comprising three or more excitons can form with distinct properties, including characteristics such as binding energy, but also correlations such as electron−hole plasma (EHP), electron−hole liquid (EHL), or quantum droplets, each of which impact the energy and rates of available recombination pathways.[26,27,31−35] EHP comprises a compressible gas of nongeminate electrons and holes that yields increasing red-shifted emission with higher density as screening increases.[17,26,32] EHL, on the other hand, presents a constant electron−hole density and produces a fixed red-shift of emission with little excitation intensity dependence.[26,27,34] Quantum droplets[26,31] describe EHL puddles that importantly feature size-dependent screening and yield progressively red-shifted emission as liquid-like droplet size (and thus, screening) increases upon elevation of pump intensity, where such states can be short-lived in direct gap semiconductors like GaAs.[31,33]

Under conditions where the spatial separation of excitons becomes comparable to the exciton size,[21] a blue shift conveying a Mott transition is expected as increased Coulomb screening reduces exciton binding energy and leads to uncorrelated band-edge charge carriers. However, the small size of excitons owing to low dielectric screening has prevented the direct observation of such a transition for CdSe NPLs.[21,36] Lack of an observable bipolar, free-carrier plasma has led to suggestions that, instead, a biexciton gas may form that could serve to largely maintain optical amplification properties at high excitation intensity.[37] Competition between a Mott transition and bandgap renormalization has been described for semiconductors, including bulk CdSe at low temperature[38] and GaAs quantum wells,[28,31] as well as in-transition metal dichalcogenides (TMDs) that in each case afford spectral red-shifting owing to EHP or EHL.[17,27,31,34,39,40]

This report describes the photophysical response of CdSe NPL films under controlled-intensity optical excitation as a function of the temperature. First, we find that the biexcitonic ASE threshold decreases by anywhere between a factor of 2 to 10 upon cooling from 298 to 5 K for neat 4 or 5 ML CdSe NPL films, depending on the characteristics of the room temperature film ASE threshold. Additionally, for neat films cooled to 200 K or below, we are able to observe strong emission at progressively redder wavelengths upon pump fluence elevation above the biexciton ASE threshold. To discern the origin of this red-shifted emission, we purposely impede ASE and dilute NPLs into an inert polymer that increases the NPL−NPL average separation to ascertain whether the red-shifted emission arises from independent particles. In these polymer-diluted films, both biexcitonic ASE and the additional red-shifted emission are suppressed for otherwise identical or even more intense pumping conditions. Our findings suggest that the red-shifted emission arises due to stimulated emission where individual particles spontaneously radiate too weakly for distinct, direct observation. In particular, the requirement of reduced temperature to produce red-shifted emission for neat films suggests that quantum droplet states likely form with a Coulomb binding energy less than the 25 meV available at room temperature and closer to ∼17 meV, corresponding to the temperature where red-shifted emission is observed. However, the nonlinear nature of the observed signal complicates the analysis of the produced polyexciton population. The red-shifted emission is inconsistent with both bandgap renormalization and EHP formation, each of which should not yield the observed sensitivity to sample temperature. This work offers insights regarding the impacts of temperature-dependent features of NPLs as well as polyexciton photophysics in 2D semiconductor NPL solids.

RESULTS AND DISCUSSION

Temperature Dependence of Biexcitonic Amplified Spontaneous Emission. Previous reports have explored means to reduce the optical gain threshold in NPLs that take advantage of their 2D particle shape (Figure S1) and emergent properties such as a putative giant oscillator strength transition, in addition to the growth of core−shell heterostructures.[5,41,42] We study the influence of temperature reduction on the ASE threshold for multiple reasons. Fundamentally, reduced phonon population at reduced temperature focuses electronic carrier populations into a narrower range of energies, which manifests as a smaller homogeneous PL line width[3] (also apparent in Figure S2). This transition narrowing occurs in addition to an overall blue shift of the band-edge for II−VI semiconductors, with the latter owing to the well-known Varshni relation[2,43] and is important, especially considering the continuous density of states that is accessible in these structures. Moreover, we recently showed that multiexcitons radiate more rapidly upon temperature reduction in CdSe NPLs,[44] suggesting the reduced competition with deleterious nonradiative Auger recombination for low temperatures. The spectroscopic appearance of trions at temperatures below ∼100 K as a lower energy emission feature[14−16] may also contribute to gain threshold reduction, as individual charges can block ground state absorption and effectively lower local band-edge state degeneracy.[45] Because biexciton binding energies for the NPL thicknesses studied herein are comparable to room temperature thermal energy, an increased population of biexcitons is expected at temperatures below ambient that can also reduce threshold.[40]

As shown in Figure 1a for 4 ML CdSe NPLs, the biexcitonic ASE threshold of neat films was first evaluated at 298 K using stripe excitation. At low pump intensity, spontaneous PL appears as a single peak (center at 523 nm = 2.371 eV, fwhm = 10.7 nm = 48.6 meV; we note that line width of the neat film exceeds that observed for a colloidal dispersion in Figure S1d). Upon increasing pump intensity for this film to 180 $\mu J/cm^2$,

https://doi.org/10.1021/acsnano.3c13170
ACS Nano XXXX, XXX, XXX−XXX

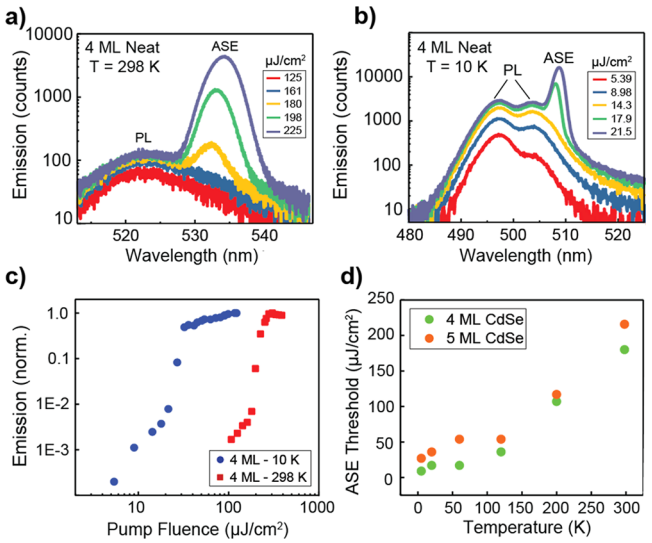

Figure 1. Amplified spontaneous emission threshold as a function of temperature. (a) Emission (PL and ASE) measured from a neat film of 4 monolayer NPLs at 298 K and (b) at 10 K. (c) Comparison of light emission intensity versus pump fluence at 298 and 10 K plotted at 533 and 508 nm, respectively. The ASE threshold values here differ by approximately 1 order of magnitude (~10-fold reduction for lower temperature). A smaller difference of ~2×, but the same general trend, was observed for films with lower room temperature thresholds (see Figure S4). (d) ASE threshold versus temperature for 4- and 5-monolayer neat NPL films derived from data similar to panels (a) and (b).

the emission redshifts (533 nm center, 44.5 meV red-shifted relative to PL), narrows (ASE band fwhm = 24.0 meV; Figure S2), and increases in intensity with a superlinear dependence on pump fluence, consistent with well-reported biexcitonic ASE.[1,4,5,33] Biexciton binding energy paired with reabsorption from a small Stokes shift give rise to the observed red-shift compared to PL energy.[9] When the film is cooled to 10 K (Figure 1b), the onset of ASE for the exact same film region occurs at a significantly lower fluence between 14 and 17.9 $\mu J/cm^2$ with an ASE band centered near 508 nm, indicating a 10-fold threshold reduction in comparison to room temperature (Figure 1c), as well as a reduced ASE line width (fwhm = 9.6 meV). Measurements were also carried out for 5 ML NPL samples and similarly exhibited an ~8-fold threshold reduction compared to room temperature (Figure S3). ASE threshold was evaluated across a series of temperatures and showed a rather systematic temperature dependence (Figure 1d), which we attribute to two main factors. Intrinsically, reduced phonon broadening narrows population distribution of the emitting states and radiative rates of biexcitons in CdSe NPLs increase relative to Auger recombination at reduced temperatures[44] both of which support the ASE threshold reduction. Notably, because biexciton binding energies are comparable to thermal energy at 298 K, some of the threshold reduction upon cooling arises from increased formation of a biexciton population commensurate with reduction of free exciton population, where only the former contribute to ASE.

Importantly, significant variation in biexcitonic ASE threshold is commonly observed at room temperature as previously reported by She et al.[5] and depends on sample features such as film optical scattering losses and NPL carrier trapping rates. Multiple regions of the same film in regions that appeared similar in optical density yielded a consistent threshold within ~15−20%, but different films and different synthetic batches of NPLs gave rise to variations such as that shown in Figure S4c. Preparation of NPL films with significantly reduced biexcitonic ASE threshold at room temperature (here as low as 12.3 $\mu J/cm^2$) also present reduced ASE threshold upon cooling, but by

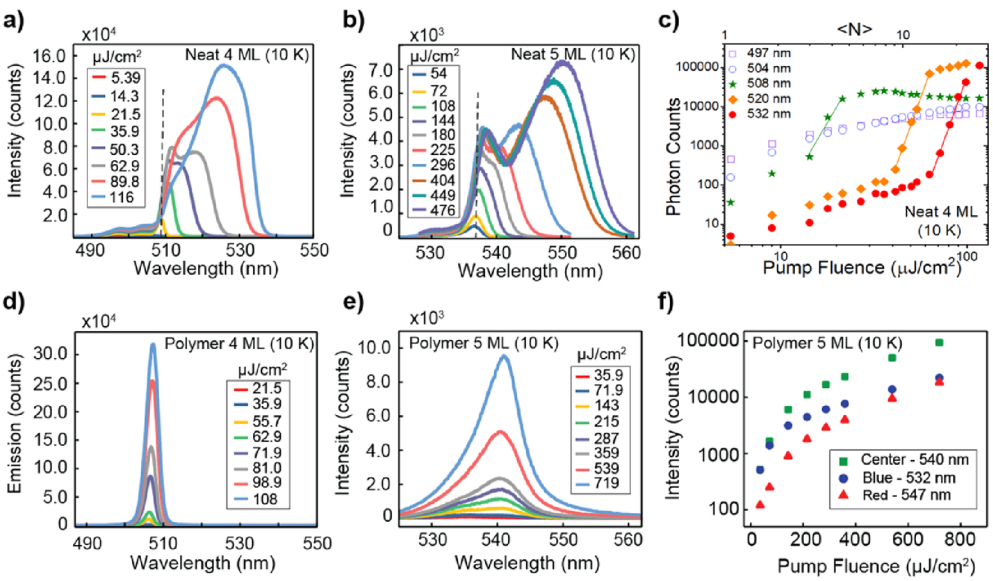

Figure 2. Elevated pump fluence measurements for neat and polymer-diluted films. (a) Emission from neat films of 4 ML NPLs and (b) 5 ML NPLs versus pump intensity at 10 K. Dashed vertical lines in (a) and (b) represent biexciton ASE center wavelengths just above threshold (508.6 and 536.5 nm, respectively). (c) Pump-fluence dependence of wavelength-resolved spontaneous PL, biexciton ASE (508 nm) and "red feature" emission from a 4 ML NPL neat film at 10 K. The average number of photons absorbed per excited nanoparticle, $\langle N \rangle$, was calculated using an absorption coefficient of 4.0×10^{-14} cm^{-2} for the 400 nm pump wavelength. (d) Emission from polymer-diluted films of 4 ML NPLs and (e) 5 ML NPLs versus pump intensity at 10 K. (f) Fluence-dependent emission at specified wavelengths for a polymer-diluted 5 ML NPL film.

https://doi.org/10.1021/acsnano.3c13170
ACS Nano XXXX, XXX, XXX−XXX

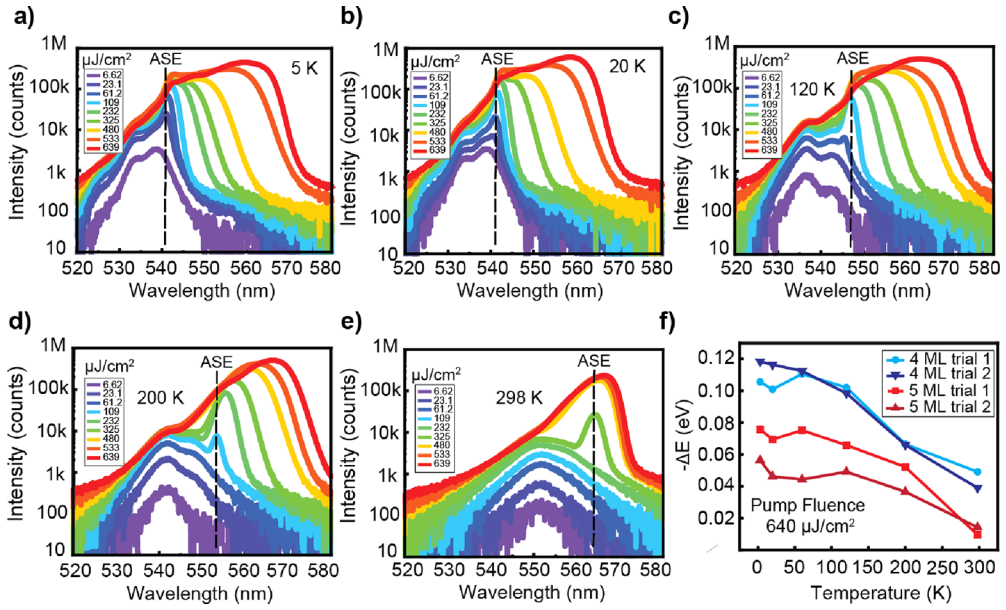

Figure 3. Temperature and fluence dependence of polyexciton emission. (a–e) 5 ML CdSe NPL neat film excited at indicated fluences for 5, 20, 120, 200, and 298 K, respectively. Above ~200 K the emission from polyexcitons is no longer prominent and only ASE is distinct (panels e and f). The extent of red-shifting at high pump intensity decreases with temperature elevation and is not appreciably red-shifted at 298 K. (f) Calculated maximum spectral shift obtained when comparing biexcitonic ASE at threshold and highest-investigated pump fluence polyexciton signal (at the center peak wavelength measured for 640 μJ/cm^2 pump intensity), $\Delta E = E_{ASE} - E_{PE,639\mu J/cm^2}$.

a smaller factor of just under 2 (see Figure S4). Because optical quality of the films likely does not improve with temperature reduction, reduced carrier trapping in addition to narrowing of transition line widths and increased biexciton (versus free exciton) population each reasonably reduce ASE threshold. Notably, both the low threshold and high threshold films approach similar biexcitonic ASE thresholds at a cryogenic temperature in this work.

Red-Shifted, Intense Light Output from Quantum Droplet Amplified Stimulated Emission. Excitation intensities that exceed the biexciton ASE threshold were initially investigated to characterize the ASE saturation behavior as a function of temperature. However, rather than observing simple saturation behavior, as has been previously reported at room temperature (which also permits the evaluation of absorption cross section and thus the average number of excitations per photoexcited particle at a given excitation fluence, $\langle N \rangle$),[4,5,36,46,47] at low temperature, elevation of pump intensity above the biexciton ASE threshold yielded distinct, progressively red-shifted, emission for both 4 and 5 ML neat films (Figure 2a and b, respectively) here referred to as polyexciton (PE) emission. The PE assignment naively can be made on the basis of the calculated average number of photon absorptions per excited NPL exceeding two, but is rationalized *vide infra* as ASE from quantum droplet exciton condensate, specifically. Figure 2c displays pump-intensity-dependent behavior of light emission at several indicated wavelengths for the same 4 ML neat film at 10 K. Monitored wavelengths correspond to spontaneous PL, biexcitonic ASE, and red-shifted PE emission (shown with logarithmic plotting in Figure S5). Measurements were also carried out for 5 ML neat films and yielded similar trends for PL and ASE, respectively (Figure S5). We consider the sample-derived light output dependence on pump intensity both in terms of particular monitored wavelengths as well as total light output (see Figure S5b,d). Free exciton spontaneous PL intensity increases linearly for low fluences and then begins to saturate as the pump intensity approaches the biexciton ASE onset. Biexcitonic ASE for the neat 4 ML NPL, monitored at 509 nm is observed at 17.9 μJ/cm^2, saturates with pump intensity elevation near ~32 μJ/cm^2, and then unexpectedly begins to decrease in intensity for fluences above ~63 μJ/cm^2. The biexcitonic ASE intensity decrease likely occurs due to competition with further red-shifted PE emission that begins to become discernible above ~40 μJ/cm^2 at 10 K. Similar trends occur for the 5 ML neat film. Total light output, integrating all emitted photons, shows an approximately linear trend at lower powers, then increases with the square or even cube of pump intensity at the higher fluences studied relating the appreciable influence stimulated emission processes impart on the nanoplatelets. The wavelength-resolved fluence dependences relate that the distribution of stimulated emission species evolves despite the more simple trend line of total light output.

In similarity to highly excited 2D MoS_2,[17,34] large red shifts at high pump intensity reasonably derive from either polyexciton EHP or polyexciton quantum droplets, both of which would feature dependence of emission wavelength on exciton density.[26,27,31,33] Conversely, the EHL, with a rather constant exciton density, would lack continuous wavelength shifting with pump fluence. PE species might be expected to spontaneously radiate for collections of isolated NPLs irrespective of NPL density in a film, whereas a high chromophore density is required for development of stimulated emission, given the typical tens-of-picosecond lifetimes of multiexciton states in simple nanostructures.

Other possible sources of transiently red-shifted emission we considered include Auger-heating of particles, wherein expanded NPL crystal lattices or even transiently disordered lattices might spontaneously radiate at lower energy.[36] To investigate such possible origins, we diluted NPLs into an inert polymer host, poly(butyl methacrylate-*co*-isobutyl-methacrylate) (see Methods), and examined the resultant films. Optical

https://doi.org/10.1021/acsnano.3c13170
ACS Nano XXXX, XXX, XXX−XXX

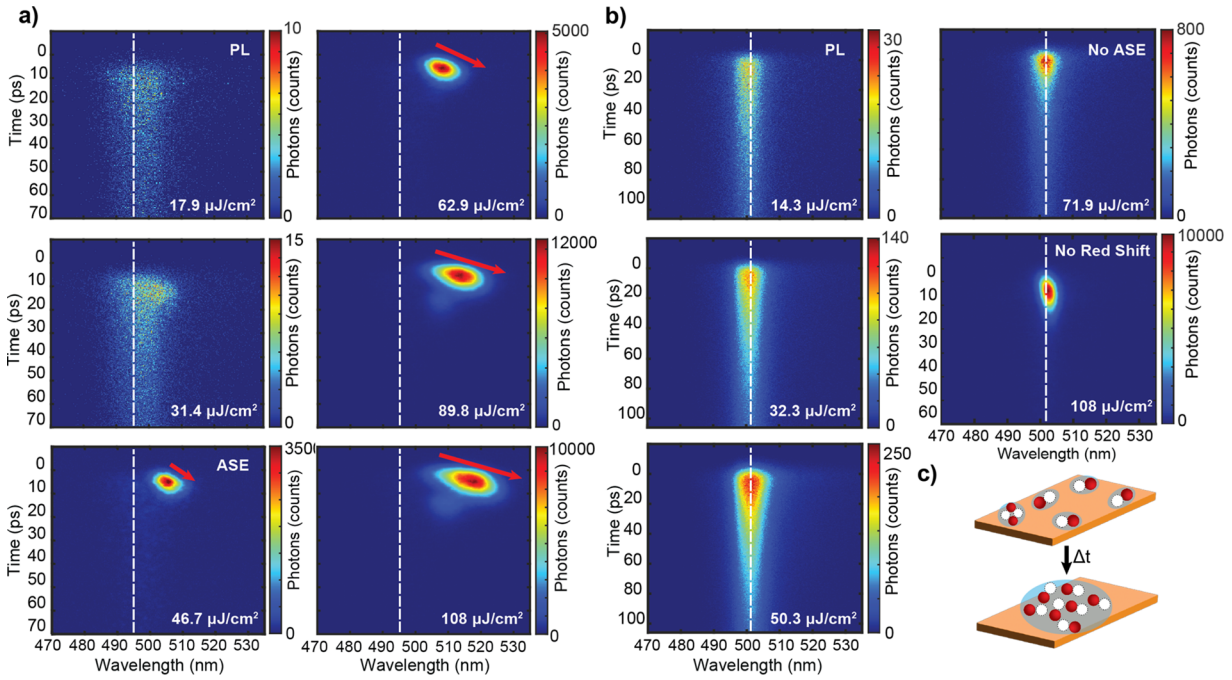

Figure 4. Time-resolved spectral dynamics at 10 K for neat and polymer-diluted 4 ML NPL films. (a, b) Streak camera dynamics recorded for a series of excitation fluences at 10 K both for (a) neat and (b) polymer-diluted 4-ML CdSe NPL films. Both films showed a decrease in emission lifetime when pump fluence is increased, however, only emission from the neat film shows emergence of a red-shifted feature, which appears to continue to red shift with delay time after the pump before it is depleted. Note that photon count scales differ with investigated pump fluence. (c) Within an intensely excited nanoplatelet, excitons form polyexciton quantum droplets owing to a binding energy in addition to that of the biexciton. Once formed, these can undergo amplified stimulated emission.

pumping of the polymer-diluted NPL films under identical or even more-intensely pumped conditions as above for neat films produced neither distinct biexcitonic ASE nor a detectable, red-shifted PE feature (Figure 2d,e). Emission intensity at three wavelengths that correspond to the center, blue, or red shoulder of the diluted NPL film emission appear in Figure 2f. Suppression of biexcitonic ASE is expected with NPL dilution because emitted photons experience a lower probability of encountering a population-inverted NPL which then impedes stimulated emission.[48] Absence of detectable red-shifted emission at high pump intensity in polymer-diluted NPL films, however, is perhaps surprising since one might expect such emission arises from spontaneous radiative recombination within each individual NPL conceivably upon Auger heating or from defect states such as surface traps. Rather, this suppression of red-shifted emission in diluted films points to an NPL-density dependent origin such as stimulated emission from PE states. Time-resolved spectroscopic investigation further bolsters this interpretation (*vide infra*).

Temperature Dependence of Polyexciton Emission and Fluence-Dependent Red-Shifting. For neat films, red-shifted PE emission is only observable at temperatures below 200 K for the pump fluence range explored (Figure 3a–e). This observation is suggestive of a characteristic binding energy that, if exceeded thermally, reduces the population of the lower energy PE species. Such a picture is analogous to the equilibrium of free excitons and biexcitons,[25,37] or similar to equilibrium of free carriers and excitons in bulk semiconductors.[49] However, quantification of PE population such as with a Boltzmann distribution is challenging since partitioning into a bound PE population versus free exciton + biexciton is complicated by detection of PE states only thru amplified stimulated emission with unknown gain cross sections. The stimulated emission detection itself is, of course, nonlinear with regard to population with competition between gain and loss channels. A polyexciton forms upon association of a biexciton and at least one other exciton, which we suggest can be crudely described by an attractive binding energy of around 17 meV based upon the ~200 K activation of the red-shifted stimulated emission, and such PE states are not observed at 298 K (where the latter corresponds to 25 meV of thermal energy). Polyexcitons appear to only weakly radiate spontaneously (because they are not observed in polymer-diluted NPL films) but apparently can undergo strongly stimulated emission processes provided that photons at this energy rapidly interact with other excited NPLs. Because the PE feature exhibits a binding energy and a continuous red shift with increasing pump fluence, attribution of the lower-energy ASE feature seems consistent with the characteristics of quantum droplets rather than an incompressible EHL. Furthermore, bandgap renormalization effects would not be expected to present such temperature sensitivity[50,51] and trap state populations would not be expected to produce light amplification owing to large energy distributions combined with small oscillator strengths.

We next evaluate the PE emission maximum at 640 μJ/cm^2 (not entirely arbitrarily but because it is the highest fluence measured that affords repeatable measurement and avoids sample damage) relative to the energy of biexciton ASE measured just above the threshold to quantify the difference output photon energy between ASE and PE emission. We examine this for both 4 and 5 ML CdSe neat films at a series of temperatures (Figure 3f, see also Figure S5 for studies of a 4 ML neat film). The largest PE red-shifts relative to biexcitonic ASE measured at 5 K for the 640 μJ/cm^2 excitation fluence were 118 and 75.7 meV for 4 and 5 ML NPLs, respectively.

https://doi.org/10.1021/acsnano.3c13170
ACS Nano XXXX, XXX, XXX−XXX

Note that here we do not expressly compare the 4 and 5 ML NPL sample properties, but aim to convey that the observables are distinctly present in both NPL thicknesses.

Light-Emission Dynamics and Transient Spectral Shifting. Time- and wavelength-resolved emission for CdSe NPL samples at T = 5 K were investigated for both neat and polymer-diluted films. When detected within the plane of the film (in-plane = 90° excitation to detection angle), emission from neat films first emerges at redder wavelengths and then becomes progressively higher in energy over the course of 30 to 40 ps (Figure S7). However, we note that the waveguided emission evaluated in this detection configuration propagates in a dispersive medium with a strong optical transition at higher energy (the 1S heavy hole exciton absorption). In particular, the wavelength-dependent refractive index of a neat CdSe film is higher at 540 nm (1.875) than at 555 nm (1.85).[52] For the same excitation fluence conditions, but instead detected in the surface-normal direction relative to the film (180° relative to the pump beam, Figure 4a), bluer emission was found to precede the redder emission by about 8 ps. This measurement configuration reduces the influence of optical dispersion within the film and suggests that initially produced free excitons subsequently give rise to lower energy species of biexcitons and polyexcitons as denoted by reduced emission energy.

The time scale required to observe decreasing emission energy after excitation conveys two processes. First, quantum droplets coalesce provided that the sample temperature is similar to or less than the polyexciton binding energy. Quantum droplets next become detectable owing to stimulated emission that decreases in energy as droplets continue to become larger until they abruptly depopulate. Just ∼12 ps after arrival of the excitation pulse, no detectable red-shifted emission is detected as directly evaluated with a streak camera. Absence of longer-lived red-shifted emission is consistent with an amplified spontaneous emission process whereas, e.g., spontaneous recombination from trap states would be expected to yield long-lived recombination dynamics that are not observed. Figure 4b shows that the same NPLs diluted in polymer for progressively higher excitation intensity decay increasingly rapidly (Tables 1 and 2) as multiple electron−hole pairs are injected into individual particles but exhibit comparatively minor red-shifting associated with biexciton recombination and absence of detectable PE radiative recombination. Five ML NPL neat and diluted films respond similarly to the 4 ML films (Figure S9). Polyexcitons, thus, seem to exhibit spontaneous recombination rates that are lower than biexcitons.

Table 1. Fitted Streak Camera Dynamics for 4 ML CdSe NPL Neat and Polymer Films at 10 K for a Series of Excitation Intensities

4 ML NPL neat film		4 ML NPL polymer film	
pump fluence (μJ/cm^2)	decay constant (ps)	pump fluence (μJ/cm^2)	decay constant (ps)
5.39	28.4 ± 2.1	5.39	74.3 ± 6.3
17.9	31.8 ± 1.0	16.1	60.9 ± 2.4
32.3	23.1 ± 0.6	32.3	54.8 ± 0.8
48.5	4.1 ± 0.04	48.5	44.0 ± 0.3
62.9	3.85 ± 0.04	71.9	21.6 ± 0.3
89.8	4.49 ± 0.03	89.8	31.0 ± 0.4
107.8	5.7 ± 0.04	107.8	6.53 ± 0.08

Table 2. Fitted Streak Camera Dynamics for 5 ML CdSe NPL Neat and Polymer Films at 10 K for a Series of Excitation Intensities

5 ML NPL neat film		5 ML NPL polymer film	
pump fluence (μJ/cm^2)	decay constant (ps)	pump fluence (μJ/cm^2)	decay constant (ps)
180	40.7 ± 1.3	11	104 ± 2.2
270	4.87 ± 0.1	30	108 ± 1.6
360	3.6 ± 0.05	90	116 ± 1
500	4.5 ± 0.05	180	110 ± 0.8
700	6.1 ± 0.07	360	92.8 ± 0.6
		600	84.8 ± 0.5

CONCLUSION

We have shown that the biexciton ASE threshold decreases appreciably with reduced temperature in 2D CdSe NPLs. Elevated pump fluence at reduced sample temperature for neat NPL films gives rise to significantly red-shifted emission that is consistent with stimulated emission from polyexcitons, which we further note is consistent with quantum droplet formation and a binding energy near ∼17 meV. Light output in the form of both biexciton ASE and PE emissions is suppressed upon dilution in a polymer, which highlights NPL-density dependence for both processes. Time- and wavelength-dependent probing indicates that the scattered emission normal to the film initially occurs at higher energy and then rapidly red-shifts, provided the sample temperature is low enough, as quantum droplets form. These studies reveal stimulated emission processes originating from quantum droplet collective excitations that form in highly confined 2D semiconductors and permit pump-fluence-dependent tuning of optical amplifiers as well as a potential stepping stone in pursuit of excitonic Bose−Einstein condensates.

METHODS

NPL Synthesis, Characterization, and Film Preparation. Colloidal CdSe NPLs were synthesized using methods reported by Ithurria et al. and She et al. with minor modifications.[2−4] Transmission electron microscopy was performed on studied NPLs and provide the average lateral dimensions of the particles (see Figure S1). NPLs were centrifuged into a pellet, redispersed in methylcyclohexane (optical density ∼1.0 in a 1 mm path cell), and drop-casted onto a clean substrate. Polymer-diluted NPL films, where the polymer was poly(butyl methacrylate-*co*-isobutyl methacrylate), were produced by adding neat solution to 100 μL of polymer solution (5% weight in toluene), stirred for 10 min, and then cast as a film.

Optical Experiments. Films were mounted in a sample-in-vacuum helium cryostat and photoexcited using 400 nm, 35 fs pulses at a 100 Hz repetition rate that, for ASE measurements, were focused via a cylindrical lens to generate a ∼2 mm wide by 0.27 mm tall stripe. Absorption cross sections of the samples at the pump wavelength of 3.1 eV were taken from the literature based upon particle dimensions. The product of the wavelength-specific absorption cross-section of a nanoparticle (σ, in cm^{-2}; typically ∼1 × 10^{-13} cm^{-2} for a CdSe NPL[47]) and the pump intensity (j, in photons/cm^2/pulse) yield the average number of photons absorbed per nanoparticle ($\langle N \rangle = \sigma j$) corresponding to the number of initially generated excitons per particle. Except where noted, emission was collected within the plane of the film (90° to the pump) and directed either to a CCD or to a streak camera. Detection geometry instances that are noted was altered to examine emission at 180° relative to the pump beam with

https://doi.org/10.1021/acsnano.3c13170
ACS Nano XXXX, XXX, XXX−XXX

reduced influence of temporal chirp within the dispersive medium of the film.

ASSOCIATED CONTENT

Supporting Information

The Supporting Information is available free of charge at https://pubs.acs.org/doi/10.1021/acsnano.3c13170.

Nanocrystal synthesis and film preparation, static and time-resolved photoluminescence method, transmission electron microscopy, and static and time-resolved pump-power-dependent emission measurements (PDF)

AUTHOR INFORMATION

Corresponding Author

Richard D. Schaller − *Department of Chemistry and International Institute for Nanotechnology, Paula Trienens Institute for Sustainability and Energy, Northwestern University, Evanston, Illinois 60208, United States; Center for Nanoscale Materials, Argonne National Laboratory, Lemont, Illinois 60439, United States;* orcid.org/0000-0001-9696-8830; Email: schaller@anl.gov, schaller@northwestern.edu

Authors

Nicolas E. Watkins − *Department of Chemistry, Northwestern University, Evanston, Illinois 60208, United States;* orcid.org/0000-0002-0417-7909

Benjamin T. Diroll − *Center for Nanoscale Materials, Argonne National Laboratory, Lemont, Illinois 60439, United States;* orcid.org/0000-0003-3488-0213

Kali R. Williams − *Department of Chemistry, Northwestern University, Evanston, Illinois 60208, United States*

Yuzi Liu − *Center for Nanoscale Materials, Argonne National Laboratory, Lemont, Illinois 60439, United States;* orcid.org/0000-0002-8733-1683

Chelsie L. Greene − *Department of Chemistry, Northwestern University, Evanston, Illinois 60208, United States*

Michael R. Wasielewski − *Department of Chemistry and International Institute for Nanotechnology, Paula Trienens Institute for Sustainability and Energy, Northwestern University, Evanston, Illinois 60208, United States;* orcid.org/0000-0003-2920-5440

Complete contact information is available at: https://pubs.acs.org/10.1021/acsnano.3c13170

Author Contributions

NPL synthesis was performed by N.E.W., B.T.D., K.R.W., and C.L.G. and film preparation was performed by N.E.W. and R.D.S. Electron microscopy was performed by N.E.W. and Y.L. Optical measurements and data analysis were performed by N.E.W., M.R.W., and R.D.S. All authors contributed to the writing of the manuscript.

Notes

The authors declare no competing financial interest.

ACKNOWLEDGMENTS

This work was supported by the National Science Foundation MSN-1808590 and the National Science Foundation Graduate Research Fellowship Program under Grant No. DGE-1324585 (N.E.W.). Use of the Center for Nanoscale Materials, an Office of Science user facility, was supported by the U.S. Department of Energy, Office of Science, Office of Basic Energy Sciences, under Contract No. DE-AC02-06CH11357. This work was supported by the U.S. Department of Energy, Office of Science, Office of Basic Energy Sciences under Award DE-FG02-99ER14999 (C.L.G. and M.R.W.). This work made use of the EPIC, Keck-II, and/or SPID facilties of Northwestern University's NUANCE Center, which has received support from the Soft and Hybrid Nanotechnology Experimental (SHyNE) Resource (NSF ECCS-1542205); the MRSEC program (NSF DMR1121262) at the Materials Research Center; the International Institute for Nanotechnology (IIN); the Keck Foundation; and the State of Illinois, through the IIN.

REFERENCES

(1) Guzelturk, B.; Kelestemur, Y.; Olutas, M.; Delikanli, S.; Demir, H. V. Amplified Spontaneous Emission and Lasing in Colloidal Nanoplatelets. *ACS Nano* **2014**, *8*, 6599−6605.

(2) Ithurria, S.; Dubertret, B. Quasi 2D colloidal CdSe platelets with thicknesses controlled at the atomic level. *J. Am. Chem. Soc.* **2008**, *130*, 16504−16505.

(3) Ithurria, S.; Tessier, M.; Mahler, B.; Lobo, R.; Dubertret, B.; Efros, A. L. Colloidal nanoplatelets with two-dimensional electronic structure. *Nat. Mater.* **2011**, *10*, 936−941.

(4) She, C.; Fedin, I.; Dolzhnikov, D. S.; Dahlberg, P. D.; Engel, G. S.; Schaller, R. D.; Talapin, D. V. Red, Yellow, Green, and Blue Amplified Spontaneous Emission and Lasing Using Colloidal CdSe Nanoplatelets. *ACS Nano* **2015**, *9*, 9475−9485.

(5) She, C.; Fedin, I.; Dolzhnikov, D. S.; Demortière, A.; Schaller, R. D.; Pelton, M.; Talapin, D. V. Low-threshold stimulated emission using colloidal quantum wells. *Nano Lett.* **2014**, *14*, 2772−2777.

(6) Guzelturk, B.; Pelton, M.; Olutas, M.; Demir, H. V. Giant modal gain coefficients in colloidal II-VI nanoplatelets. *Nano Lett.* **2019**, *19*, 277−282.

(7) Watkins, N. E.; Guan, J.; Diroll, B. T.; Williams, K. R.; Schaller, R. D.; Odom, T. W. Surface Normal Lasing from CdSe Nanoplatelets Coupled to Aluminum Plasmonic Nanoparticle Lattices. *J. Phys. Chem. C* **2021**, *125*, 19874−19879.

(8) Yang, Z.; Pelton, M.; Fedin, I.; Talapin, D. V.; Waks, E. A room temperature continuous-wave nanolaser using colloidal quantum wells. *Nat. Commun.* **2017**, *8*, 143.

(9) Grim, J. Q.; Christodoulou, S.; Di Stasio, F.; Krahne, R.; Cingolani, R.; Manna, L.; Moreels, I. Continuous-wave biexciton lasing at room temperature using solution-processed quantum wells. *Nature Nanotechnol.* **2014**, *9*, 891−895.

(10) Baghani, E.; O'Leary, S. K.; Fedin, I.; Talapin, D. V.; Pelton, M. Auger-limited carrier recombination and relaxation in CdSe colloidal quantum wells. *J. Phys. Chem. Lett.* **2015**, *6*, 1032−1036.

(11) Kunneman, L. T.; Tessier, M. D.; Heuclin, H.; Dubertret, B.; Aulin, Y. V.; Grozema, F. C.; Schins, J. M.; Siebbeles, L. D. Bimolecular Auger recombination of electron-hole pairs in two-dimensional CdSe and CdSe/CdZnS core/shell nanoplatelets. *J. Phys. Chem. Lett.* **2013**, *4*, 3574−3578.

(12) Philbin, J. P.; Brumberg, A.; Diroll, B. T.; Cho, W.; Talapin, D. V.; Schaller, R. D.; Rabani, E. Area and thickness dependence of Auger recombination in nanoplatelets. *J. Chem. Phys.* **2020**, *153*, 054104.

(13) Ma, X.; Diroll, B. T.; Cho, W.; Fedin, I.; Schaller, R. D.; Talapin, D. V.; Gray, S. K.; Wiederrecht, G. P.; Gosztola, D. J. Size-dependent biexciton quantum yields and carrier dynamics of quasi-two-dimensional core/shell nanoplatelets. *ACS Nano* **2017**, *11*, 9119−9127.

(14) Antolinez, F. V.; Rabouw, F. T.; Rossinelli, A. A.; Keitel, R. C.; Cocina, A.; Becker, M. A.; Norris, D. J. Trion emission dominates the low-temperature photoluminescence of CdSe nanoplatelets. *Nano Lett.* **2020**, *20*, 5814−5820.

(15) Peng, L.; Otten, M.; Hazarika, A.; Coropceanu, I.; Cygorek, M.; Wiederrecht, G. P.; Hawrylak, P.; Talapin, D. V.; Ma, X. Bright trion

emission from semiconductor nanoplatelets. *Physical Review Materials* **2020**, *4*, 056006.
(16) Shornikova, E. V.; Yakovlev, D. R.; Biadala, L.; Crooker, S. A.; Belykh, V. V.; Kochiev, M. V.; Kuntzmann, A.; Nasilowski, M.; Dubertret, B.; Bayer, M. Negatively charged excitons in CdSe nanoplatelets. *Nano Lett.* **2020**, *20*, 1370−1377.
(17) Bataller, A. W.; Younts, R. A.; Rustagi, A.; Yu, Y.; Ardekani, H.; Kemper, A.; Cao, L.; Gundogdu, K. Dense electron-hole plasma formation and ultralong charge lifetime in monolayer MoS2 via material tuning. *Nano Lett.* **2019**, *19*, 1104−1111.
(18) Chernikov, A.; Berkelbach, T. C.; Hill, H. M.; Rigosi, A.; Li, Y.; Aslan, B.; Reichman, D. R.; Hybertsen, M. S.; Heinz, T. F. Exciton binding energy and nonhydrogenic Rydberg series in monolayer WS 2. *Phys. Rev. Lett.* **2014**, *113*, 076802.
(19) Feng, J.; Qian, X.; Huang, C.-W.; Li, J. Strain-engineered artificial atom as a broad-spectrum solar energy funnel. *Nat. Photonics* **2012**, *6*, 866−872.
(20) Benchamekh, R.; Gippius, N. A.; Even, J.; Nestoklon, M.; Jancu, J.-M.; Ithurria, S.; Dubertret, B.; Efros, A. L.; Voisin, P. Tight-binding calculations of image-charge effects in colloidal nanoscale platelets of CdSe. *Phys. Rev. B* **2014**, *89*, 035307.
(21) Brumberg, A.; Harvey, S. M.; Philbin, J. P.; Diroll, B. T.; Lee, B.; Crooker, S. A.; Wasielewski, M. R.; Rabani, E.; Schaller, R. D. Determination of the in-plane exciton radius in 2D CdSe nanoplatelets via magneto-optical spectroscopy. *ACS Nano* **2019**, *13*, 8589−8596.
(22) Shornikova, E. V.; Yakovlev, D. R.; Gippius, N. A.; Qiang, G.; Dubertret, B.; Khan, A. H.; Di Giacomo, A.; Moreels, I.; Bayer, M. Exciton Binding Energy in CdSe Nanoplatelets Measured by One-and Two-Photon Absorption. *Nano Lett.* **2021**, *21*, 10525−10531.
(23) Ji, B.; Rabani, E.; Efros, A. L.; Vaxenburg, R.; Ashkenazi, O.; Azulay, D.; Banin, U.; Millo, O. Dielectric confinement and excitonic effects in two-dimensional nanoplatelets. *ACS Nano* **2020**, *14*, 8257−8265.
(24) Pelton, M.; Ithurria, S.; Schaller, R. D.; Dolzhnikov, D. S.; Talapin, D. V. Carrier cooling in colloidal quantum wells. *Nano Lett.* **2012**, *12*, 6158−6163.
(25) Geiregat, P.; Tomar, R.; Chen, K.; Singh, S.; Hodgkiss, J. M.; Hens, Z. Thermodynamic equilibrium between excitons and excitonic molecules dictates optical gain in colloidal cdse quantum wells. *J. Phys. Chem. Lett.* **2019**, *10*, 3637−3644.
(26) Jeffries, C. D. Electron-Hole Condensation in Semiconductors: Electrons and holes condense into freely moving liquid metallic droplets, a plasma phase with novel properties. *Science* **1975**, *189*, 955−964.
(27) Keldysh, L. The electron-hole liquid in semiconductors. *Contemporary Physics* **1986**, *27*, 395−428.
(28) Kim, J.; Wake, D.; Wolfe, J. Thermodynamics of biexcitons in a GaAs quantum well. *Phys. Rev. B* **1994**, *50*, 15099.
(29) Martin, P. I.; Panuganti, S.; Portner, J. C.; Watkins, N. E.; Kanatzidis, M. G.; Talapin, D. V.; Schaller, R. D. Excitonic Spin-Coherence Lifetimes in CdSe Nanoplatelets Increase Significantly with Core/Shell Morphology. *Nano Lett.* **2023**, *23*, 1467−1473.
(30) Achermann, M.; Hollingsworth, J. A.; Klimov, V. I. Multi-excitons confined within a subexcitonic volume: Spectroscopic and dynamical signatures of neutral and charged biexcitons in ultrasmall semiconductor nanocrystals. *Phys. Rev. B* **2003**, *68*, 245302.
(31) Almand-Hunter, A.; Li, H.; Cundiff, S.; Mootz, M.; Kira, M.; Koch, S. W. Quantum droplets of electrons and holes. *Nature* **2014**, *506*, 471−475.
(32) Hendry, E.; Koeberg, M.; Bonn, M. Exciton and electron-hole plasma formation dynamics in ZnO. *Phys. Rev. B* **2007**, *76*, 045214.
(33) Turner, D. B.; Nelson, K. A. Coherent measurements of high-order electronic correlations in quantum wells. *Nature* **2010**, *466*, 1089−1092.
(34) Yu, Y.; Bataller, A. W.; Younts, R.; Yu, Y.; Li, G.; Puretzky, A. A.; Geohegan, D. B.; Gundogdu, K.; Cao, L. Room-temperature electron-hole liquid in monolayer MoS2. *ACS Nano* **2019**, *13*, 10351−10358.
(35) Steele, A.; McMullan, W.; Thewalt, M. Discovery of polyexcitons. *Phys. Rev. Lett.* **1987**, *59*, 2899.
(36) Diroll, B. T.; Brumberg, A.; Schaller, R. D. Gain roll-off in cadmium selenide colloidal quantum wells under intense optical excitation. *Sci. Rep.* **2022**, *12*, 1−10.
(37) Flórez, F. G.; Siebbeles, L. D. A.; Stoof, H. T. C. Biexcitons in highly excited CdSe nanoplatelets. *Phys. Rev. B* **2020**, *102*, 115302.
(38) Masumoto, Y.; Fluegel, B.; Meissner, K.; Koch, S.; Binder, R.; Paul, A.; Peyghambarian, N. Band-gap renormalization and optical gain formation in highly excited CdSe. *J. Cryst. Growth* **1992**, *117*, 732−737.
(39) Wilmington, R.; Ardekani, H.; Rustagi, A.; Bataller, A.; Kemper, A.; Younts, R.; Gundogdu, K. Fermi liquid theory sheds light on hot electron-hole liquid in 1 L- Mo S 2. *Phys. Rev. B* **2021**, *103*, 075416.
(40) Chernikov, A.; Ruppert, C.; Hill, H. M.; Rigosi, A. F.; Heinz, T. F. Population inversion and giant bandgap renormalization in atomically thin WS2 layers. *Nat. Photonics* **2015**, *9*, 466−470.
(41) Li, Q.; Liu, Q.; Schaller, R. D.; Lian, T. Reducing the Optical Gain Threshold in Two-Dimensional CdSe Nanoplatelets by the Giant Oscillator Strength Transition Effect. *J. Phys. Chem. Lett.* **2019**, *10*, 1624−1632.
(42) Erdem, O.; Foroutan, S.; Gheshlaghi, N.; Guzelturk, B.; Altintas, Y.; Demir, H. V. Thickness-Tunable Self-Assembled Colloidal Nanoplatelet Films Enable Ultrathin Optical Gain Media. *Nano Lett.* **2020**, *20*, 6459−6465.
(43) Varshni, Y. P. Temperature dependence of the energy gap in semiconductors. *Physica* **1967**, *34*, 149−154.
(44) Brumberg, A.; Watkins, N. E.; Diroll, B. T.; Schaller, R. D. Acceleration of Biexciton Radiative Recombination at Low Temperature in CdSe Nanoplatelets. *Nano Lett.* **2022**, *22*, 6997−7004.
(45) Wu, K.; Park, Y.-S.; Lim, J.; Klimov, V. I. Towards zero-threshold optical gain using charged semiconductor quantum dots. *Nat. Nanotechnol.* **2017**, *12*, 1140−1147.
(46) Tomar, R.; Kulkarni, A.; Chen, K.; Singh, S.; van Thourhout, D.; Hodgkiss, J. M.; Siebbeles, L. D. A.; Hens, Z.; Geiregat, P. Charge Carrier Cooling Bottleneck Opens Up Nonexcitonic Gain Mechanisms in Colloidal CdSe Quantum Wells. *J. Phys. Chem. C* **2019**, *123*, 9640−9650.
(47) Yeltik, A.; Delikanli, S.; Olutas, M.; Kelestemur, Y.; Guzelturk, B.; Demir, H. V. Experimental Determination of the Absorption Cross-Section and Molar Extinction Coefficient of Colloidal CdSe Nanoplatelets. *J. Phys. Chem. C* **2015**, *119*, 26768−26775.
(48) Klimov, V.; Mikhailovsky, A.; Xu, S.; Malko, A.; Hollingsworth, J.; Leatherdale, a. C.; Eisler, H.-J.; Bawendi, M. Optical gain and stimulated emission in nanocrystal quantum dots. *Science* **2000**, *290*, 314−317.
(49) D'innocenzo, V.; Grancini, G.; Alcocer, M. J.; Kandada, A. R. S.; Stranks, S. D.; Lee, M. M.; Lanzani, G.; Snaith, H. J.; Petrozza, A. Excitons versus free charges in organo-lead tri-halide perovskites. *Nat. Commun.* **2014**, *5*, 3586.
(50) Lin, Y.; Chan, Y.-h.; Lee, W.; Lu, L.-S.; Li, Z.; Chang, W.-H.; Shih, C.-K.; Kaindl, R. A.; Louie, S. G.; Lanzara, A. Exciton-driven renormalization of quasiparticle band structure in monolayer MoS 2. *Phys. Rev. B* **2022**, *106*, L081117.
(51) Ulstrup, S.; Cabo, A. G.; Miwa, J. A.; Riley, J. M.; Grønborg, S. S.; Johannsen, J. C.; Cacho, C.; Alexander, O.; Chapman, R. T.; Springate, E.; et al. Ultrafast band structure control of a two-dimensional heterostructure. *ACS Nano* **2016**, *10*, 6315−6322.
(52) Zhang, Z.; Thung, Y. T.; Chen, X.; Wang, L.; Fan, W.; Ding, L.; Sun, H. Study of Complex Optical Constants of Neat Cadmium Selenide Nanoplatelets Thin Films by Spectroscopic Ellipsometry. *J. Phys. Chem. Lett.* **2021**, *12*, 191−198.

https://doi.org/10.1021/acsnano.3c13170
ACS Nano XXXX, XXX, XXX−XXX